American Journal of Engineering Research (AJER)
e-ISSN : 2320-0847 p-ISSN : 2320-0936
Volume-3, Issue-7, pp-125-140
www.ajer.org
Research Open Access

A Novel Harmonic-Based Phase-Shifted Control Method to Regulate The Transferred Power

[1,]G.Kaladhar , [2,]Y.Narayana Rao , [3,] G.Gopala Rao

ABSTRACT: *over a wide range of load the power is regulated with high efficiency by inductively coupled power transfer system. In this paper a novel harmonic based phase-shifted control method is proposed. With this method, the resonant inverter output voltage is employed to regulate the output power. By changing the phase-shifted angle of inverter the output power is regulated. The switching frequency is much lower than the fundamental frequency which is different from conventional approaches; therefore the switching losses are very less. The principle of operation, switching strategy and the effect of dead time has all been presented. Experimental results says that the proposed power regulate method can achieve improvement at the light load condition.*

Index Terms: *Inductively coupled power transfer(ICPT), Phase-shifted control, Harmonic, power regulation, Efficiency.*

NOMENCLATURE

L_p	Total inductance of primary winding
L_s	Total inductance of secondary winding
M	Mutual inductance
C_p	Resonant capacitor on primary side
C_s	Resonant capacitor on secondary side
R_p	Total resistance of primary winding
R_s	Total resistance of secondary winding
R_L	Load resistance
R_e	Equivalent resistance of load
Z_{pk}	Self impedance of kth order harmonic component on primary side
Z_{sk}	Self impedance of kth order harmonic component on secondary side
Z_r	Reflected impedance of the secondary circuit seen by the primary side
S_1 - S_4	switching components
D_1- D_4	freewheeling diodes

D_5- D_8 diodes

C_f Filter capacitance

V_{dc} Voltage of dc input source

V_{inv} Inverter output voltage

V_{pk} Root mean square value of the kth-order harmonic component

V_{Rek} Voltage of equivalent resistance of the k^{th}-order harmonic component

I_p Inverter output current

I_{pk} Inverter output current of the kth-order harmonic component

I_{sk} Secondary winding current of the kth-order harmonic component

f_r Resonant frequency

f_s Switching frequency

ω_s Switching angular frequency

ω_r Resonant angular frequency

$\propto$ Phase shifted angle

t_d Delay time of inverter

P_{out} Output power on load

η Transfer efficiency

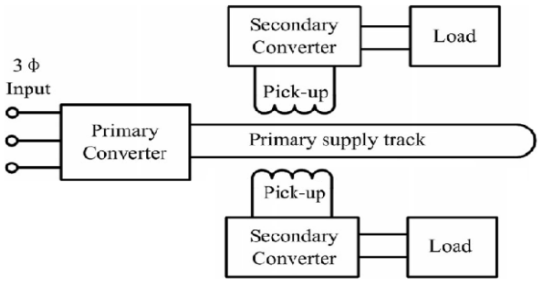

Fig.1. Basic ICPT system with multiple loads.

I. INTRODUCTION

The term inductively coupled transformer (ICPT) in general can be used to describe the power transfer between two objects that are physically un- connected. The use of contactless power is sometimes the only way of transferring power between the source and load. There are so many applications of this technology, high-power applications and low power applications. Low power applications are wireless charging of cell phones, laptops, TVs, desktops, and also in biomedical applications where as high power applications are people movers, industrial transport, automation, mining, military and aviation. but unlike low power transfer applications where the air gap between the load and source is very small and power transfer efficiency is comparatively small, in case of high power transfer the air gaps are larger and efficiency of power transfer is intended to be high as the amount of power transfer is large.ICPT system utilizes varying magnetic field at a certain frequency to couple power across an air gap to one or more secondary load systems without direct physical contact .ICPT is safe, reliable ,and flexible and environmental friendly due to electrical isolation of the

system. The movable contactless power transfer (MCPT) system is an alternative proposal for the supply of rail transit system .The MCPT system contains the ground part and vehicle part; the primary windings are powered by converter located on the ground and the secondary windings pickup the power and transfer it to load. For high power applications, it is necessary to regulate the output power of ICPT system with the load change.

The output power is regulated by changing input dc voltage but this method is simple but increases the power losses, size and cost of the power primary converter. Phase-shifted angle variation method is used to regulate the fundamental output voltage in full bridge inverter. While comparing different control methods i.e. voltage control, duty cycle control, frequency control, and phase angle control, phase angle control gives the optimal scheme under the uniform load condition.The objective of this paper is to analyze the variation of output powers in different compensation systems, first the fundamental principle of ICPT system is analysed.Then, and a harmonic model equivalent circuit for ICPT with series capacitor on both sides is built. After that, the harmonic-based phase-shifted control (HPSC) method is derived. Comparative analyses and experiments for the proposed and conventional methods are investigated. The compensation capacitance values are find out using the equations given in Table-A for different compensation topologies.

II. FUNDAMENTAL PRINCIPLE

The basic circuit diagram of ICPT system shown in fig.1. It contains a set of coils near and along the rail known as primary winding, one or more secondary winding coils beneath the vehicle. The primary converter converts three phase 50HZ ac voltage into DC voltage, then the inverter outputs high frequency ac to primary winding coil and set of high frequency magnetic field. The high frequency voltage is induced in secondary winding coils which couple with magnetic field. The secondary converter converts ac voltage to DC voltage through Diode Bridge for the load R_L.Which is a motor or inverter.In order to increase the transferred power as well as efficiency, compensation capacitors are used in the ICPT system. Basically there are four types of compensation topologies; those are series-series compensation (SS), series- parallel compensation (SP), parallel-series compensation (PS), parallel-parallel compensation (PP) as shown in following fig (a), fig (b), fig(c) and fig (d) respectively.Compensation capacitors are also used to reduce the apparent power of primary converter. If both primary and secondary compensation capacitors are connected serially, then no need to vary the capacitance with the load or the mutual inductance between primary winding and secondary winding. On the other hand the SS topology has one more advantage is that; the reflected impedance of the secondary winding on to the primary winding has only a real reflected component and no reactive component. In the conventional method, the power is transferred by fundamental component, and harmonic components are usually neglected. So, the conventional phase-shifted control is called fundamental-based phase-shifted control (FPSC) in this paper.

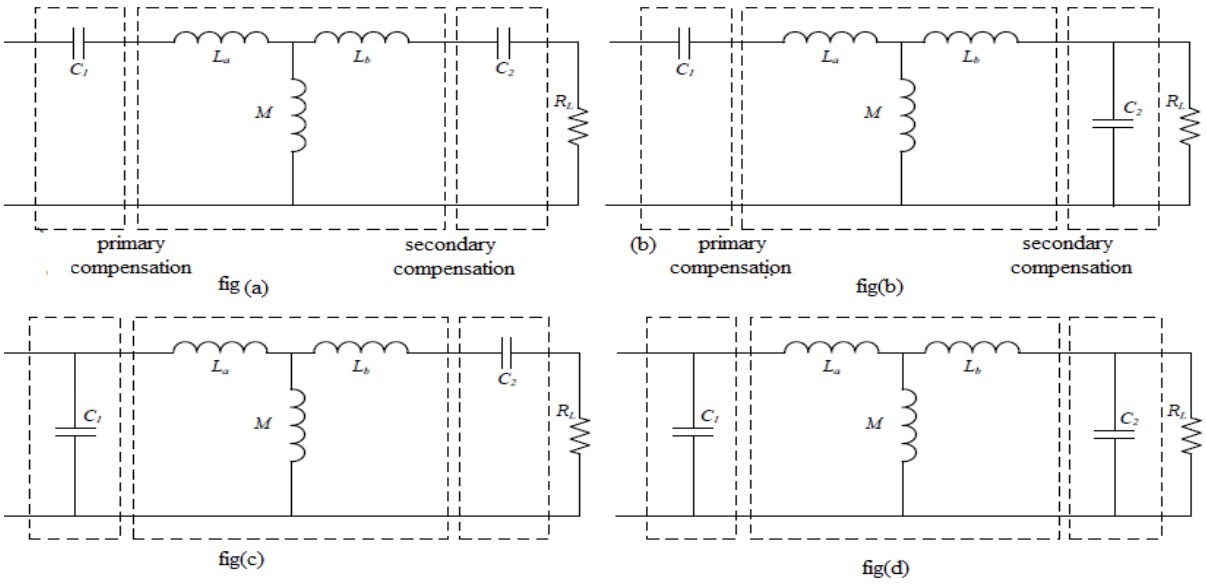

Fig.4. Compensation topologies (a) SS (b) SP (c) PS (d) PP.

TABLE-A

Topology	C_2	C_1
SS	$C_2 = \frac{1}{\omega_s^2(L_b+M)}$	$C_1 = \frac{1}{\omega_s^2(L_b+M)}$
SP	$C_2 = \frac{1}{\omega_s^2(L_b+M)}$	$C_1 = \frac{(L_b+M)^2 C_2}{(L_a+M)(L_b+M)-M^2}$
PS	$C_2 = \frac{1}{\omega_s^2(L_b+M)}$	$C_1 = \frac{(L_a+M)(L_b+M)^2 C_2^2 R_L^2}{M^4+(L_a+M)(L_b+M)R_L^2}$
PP	$C_2 = \frac{1}{\omega_s^2(L_b+M)}$	$C_1 = \frac{(L_b+M)^2((L_a+M)(L_b+M)-M^2)C_2}{((L_b+M)(L_a+M)-M^2)^2+M^4 R_L^2(L_b+M)C_2}$

To analyze the harmonic components, fast Fourier transform (FFT) of the inverter output voltage is carried out at first. Here, the dead time of inverter is not considered, the root-mean-square (RMS) value of the kth –order harmonic component of inverter output voltage is given by

$$V_{PK} = \frac{2\sqrt{2}}{k\pi}\cos\frac{k\alpha}{2} \quad (k = 1,3,5,7 \ldots\ldots). \qquad (1)$$

The fundamental model equivalent circuit of ICPT system is presented in [21]. Similarly, the *k*th-

order harmonic model is built in this paper to analyze the effect of the harmonic components as well as the fundamental to the transferred power. The harmonic model equivalent circuit with series capacitors on both sides is shown in Fig.2.

As indicated in Fig.2, the primary current I_{PK} and secondary current I_{sK} can be expressed as

$$\begin{bmatrix} I_{PK} \\ I_{SK} \end{bmatrix} = \frac{V_{pK}}{Z_{pK}Z_{sK}+(K\omega_s M)^2}\begin{bmatrix} Z_{sk} \\ jk\omega_s M \end{bmatrix} \qquad (2)$$

Where

$$\omega_s = 2\pi f_s \qquad (3)$$

$$R_e = \frac{8}{\pi^2}R_L \qquad (4)$$

$$Z_{pk} = \mathrm{j}k\omega_s L_p + \frac{1}{jk\omega_s C_P} + R_p \qquad (5)$$

$$Z_{sk} = jk\omega_s L_s + \frac{1}{jk\omega_s C_s} + R_s + R_e. \qquad (6)$$

The *k*th-order harmonic component P_{ok} in output power is expressed as

$$P_{ok} = I_{sk}^2 R_e = \frac{8\cos^2(\frac{k\alpha}{2})}{k^2\pi^2}\frac{V_{dc}^2(K\omega_s M)^2 R_e}{|Z_{pk}Z_{sk}+(k\omega_s M)^2|^2}. \qquad (7)$$

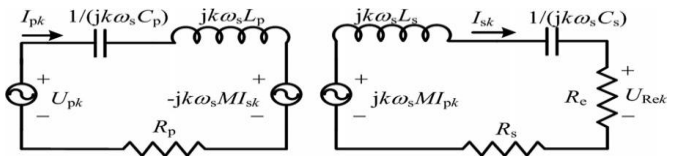

Fig.2. Harmonic model equivalent circuit of ICPT with series compensation.

III. THE HARMONIC BASED PHASE-SHIFTED CONTROL

A. The Harmonic Based Phase-Shifted Control

To transfer power in FPSC, the harmonic component of inverter output voltage is used by changing switching frequency. Where as in HPSC, to regulate output power accurately phase shifted control is used. The following are the steps to analyze the HPSC

Step-1: Harmonic components of inverter output voltage must be found out.

Step-2: Normalized value has to be introduced

We know that,

$$V_{pk} = \frac{2\sqrt{2}}{k\pi} V_{dc} \cos\frac{k\alpha}{2} \quad (K=1,3,5,\ldots\ldots\ldots\ldots) \qquad (8)$$

At, $\alpha = 0$

$$V_{p1} = \frac{2\sqrt{2}}{\pi} Vdc \qquad (9)$$

Therefore, Normalized value of k_{th} order harmonic RMS value, at phase shifted angle 'α' is

$$G_k = \frac{Vpk}{Vp1} \qquad (10)$$

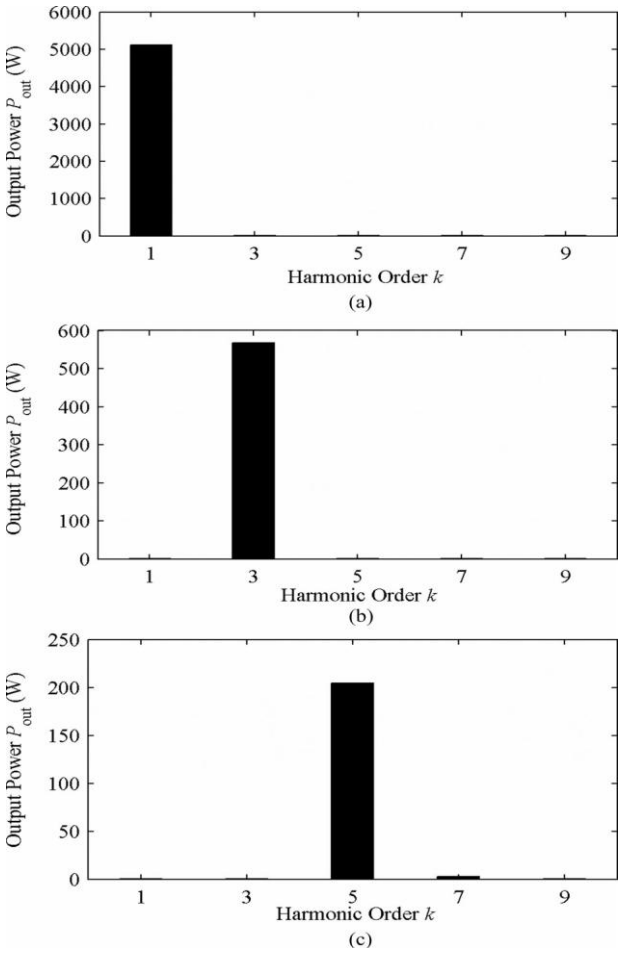

Fig.3 output power with different harmonic components under f_r = 42kHz: (a) 42kHz,(b)14kHz, and (c)8.4kHz.

$$G_k = \frac{1}{k}\cos\frac{k\alpha}{2} \quad (k=1, 3, 5 \ldots) \qquad (11)$$

Where

G_k= Normalized RMS harmonic voltage

To illustrate this method, Fig.6 shows key waveforms of the third-order harmonic-based control method. Furthermore, a half switching period in Fig.6 is subdivided into six stages and their simplified paths in different stages are shown in Fig.8.

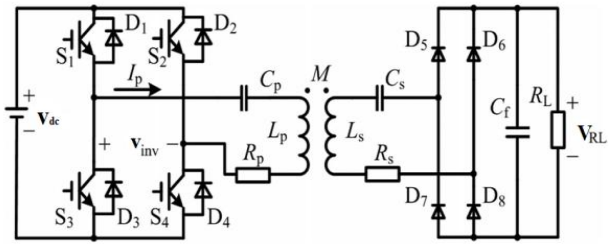

Fig.5. circuit topology of ICPT with series compensation.

Region1 [t_0 tot_1]:S_3turns OFF at t_0.from $t_0$to $t_1$the power is oscillating freely through S_2, Lp, Zr, Rp, Cp, and D_1.$V_{inv}$is equal to 0 during this stage.

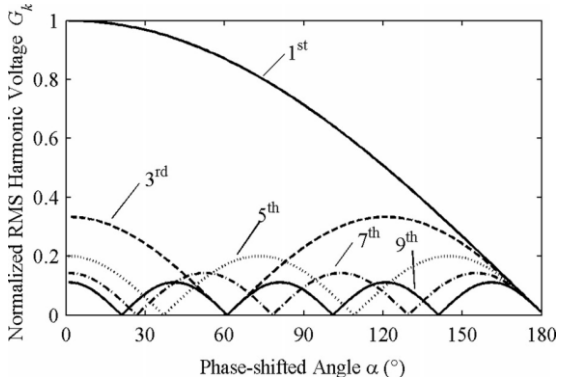

Fig.7. Normalized Value of Fundamental and Harmonic Components at Different Phase-Shifted Angle.

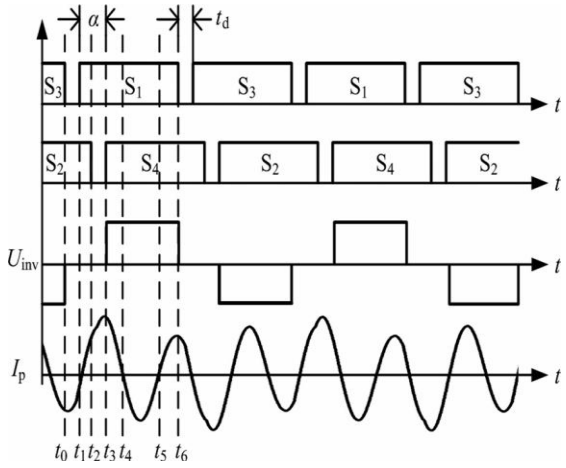

Fig.6. key waveforms of HPSC with third order harmonic.

Region2 [t_1 tot$_2$]: At t_1, S1 turns ON at zero voltage switching (ZVS) when D_1conducts. The power is oscillating freely through S_1, C_p, R_p, Zr, L_p , and D_2.

Region3 [t_2 tot$_3$]: At t_2, S_2 turns OFF at zero voltage switching (ZVS) when D_2conducts

Region4 [t_3 tot$_4$]:S_4turns ON at t_3, and D_2turns OFF at the same time. The conduction current through S_4 is same with the turning OFF current of D_2.the power is transferred from input dc source to load through S_1, C_p, R_p, Zr, L_p, and S_4.$V_{inv}$is equal to V_{dc} during this stage.

Region5[t_4 tot$_5$]:Inverter output current $I_p$crosses zero and changes its direction at t_4.the power is circulated from load to input dc source through D_4, L_p, Zr, R_p, C_p,and D_1.this stage finishes when I_p reaches zero.

Region6 [t_5 tot$_6$]:After current I_p crosses zero and changes its direction at t_5,the power is transferred from input dc source to load through S_1, C_p, R_p, Zr, L_p,and

S_4 during this stage. This stage ends when S_1turnsOFF at t_6. The other half period current directions are similar as explained above. The current I_p circulates three times during one switching period, which means lower switching losses compared with FPSC.

Switching Strategy for Harmonic Components:

From Fig.7, it is evident that several harmonic components meet the demand of low output power. The switching strategy for different order harmonic is discussed as follows.First, α_{1k} is defined as the switching phase-shifted angle from fundamental to the kth-order harmonic component. When fundamental component is at resonance, the kth-order harmonic component could be employed to transfer the same power if the phase-shifted angle is greater than α_{1k}. The maximum value of G_k is 1/k, so from the relationship G_1=1/k, α_{1k} can be expressed as

$$\alpha_{1k} = \frac{360^\circ}{\pi} arccos \frac{1}{k} \ (k = 1,3,5,7 \ldots.). \quad (12)$$

Similarly, α_{1k} is defined as switching phase-shifted angle from the kth-order harmonic to (k+2)th-order harmonic. When the kth-order harmonic is at resonance, if the phase-shifted angle is greater than α_k, then (k+2)th-order harmonic can be used to transfer same capacity of power. It means the reasonable phase-shifted angle range

$$\alpha_K = \frac{360^\circ}{K\pi} arccos \frac{k}{k+2} \ (k = 1,3,5,7 \ldots.) \quad (13)$$

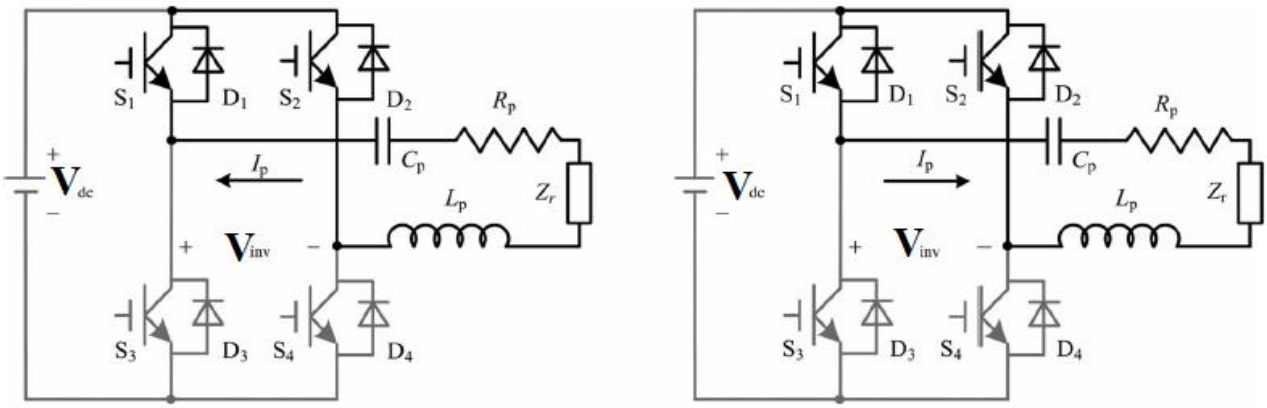

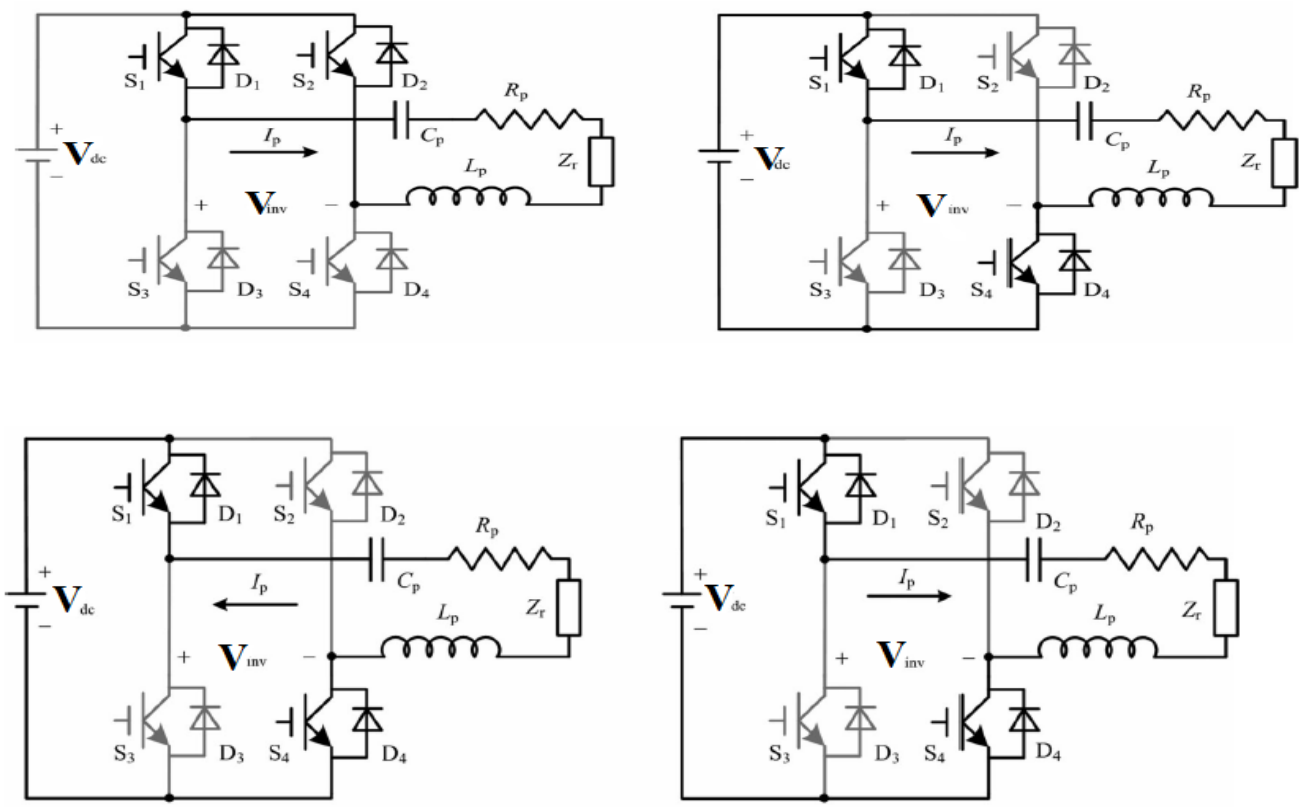

Fig.8. simplified paths of HPSC with third-order in half switching period.

of k[th]- order harmonic can be 0 to α_k. From the relationship G_k=1/(k+2), α_k can be expressed as

The switching phase-shifted angles for fundamental and harmonic components are shown in Table II. Generally, by ignore the components which are not at resonance, the normalized value of output power is

$$G_{Pk} = G_k^2 = \frac{1}{k^2} cos^2 \frac{k\alpha}{2} \quad \text{(k=1,3,5,7…..).} \qquad (14)$$

TABLE –I

SIMULATION AND EXPERIMENTAL PARAMETERS

symbol	value	symbol	value
V_{dc}(v)	90	$R_P(\Omega)$	0.1
L_P(µH)	39	$R_L(\Omega)$	20
L_S(µH)	149	$C_P(\mu F)$	0.36
$M(\mu H)$	16	$C_S(\mu F)$	0.09
$R_S(\Omega)$	0.2	$f_r(kHz)$	42

Effect of Dead Time

The dead time is necessary to avoid current passing directly through any bridge arm of an inverter. Because it will bring some effect to duty width, it must be considered especially for high frequency switching.

TABLE-II

SWITCHING PHASE SHIFTED ANGLES FOR FUNDAMENTAL AND HARMONIC

Harmonic Order	$\alpha_{1k}(^\circ)$	$\alpha_k(^\circ)$
1	0	141.1
3	141.1	35.4
5	156.9	17.8
7	163.6	11.1
9	167.2	7.8
k	$\frac{360^\circ}{\pi} arccos\frac{1}{k}$	$\frac{360^\circ}{k\pi} arccos\frac{k}{k+2}$

For example the effective duty width will be decreased from 50% to 41.6% if dead time is 2μs and switching frequency is 40 kHz, which results in decreased in maximum output power. Here α_{kd} is defined as equilent phase-shifted angle of dead time for k_{th} order harmonic in HPSC, and it is expressed as

$$\alpha_{kd} = \frac{t_d f_r}{k} 360 \ (k = 1,3,5,7 \dots .). \quad (15)$$

Considering the dead time effect, the equations with phase shifted angle α will be updated. Taking V_{pk} as an example,(1) is updated as

$$v'_{pk} = \frac{2\sqrt{2}}{k\pi} v_{dc} \cos\frac{k(\alpha+\alpha_{kd})}{2} \ (k = 1,3,5,7 \dots \dots). \quad (16)$$

Besides, the switching phase-shifted angle will be up dated as

$$\alpha'_{1k} = \frac{360^\circ}{\pi} arccos\frac{1}{k} - t_d f_r 360 \ (k = 1,3,5,7 \dots .). \quad (17)$$

$$\alpha'_{k} = \frac{360^\circ}{k\pi} arccos\frac{k}{k+2} - t_d f_r 360 \ (k = 1,3,5,7 \dots .). \quad (18)$$

It is evident that the phase shifted angle for the maximum value of $v'_{pk} \ (k = 3,5,7 \dots)$ is $\frac{360}{k} - \alpha_{kd}$ instead of zero. The lost phase-shifted angle range due to the dead time can be replaced by $\frac{360}{k} - \alpha_{kd} \sim \frac{360}{k}$.

IV. EXPERIMENTAL RESULTS

A. Experimental setup

In order to verify the validity of HPSC power regulation method, experiments have been implemented on a prototype of movable contactless power supply system for rail transit system. The prototype consists of a contactless transformer and two converters. The contactless transformer contains long primary winding and short secondary winding. The former is fixed on ground along the track, and the latter is fixed on the movable vehicle. The converter topology adopted is same as that in fig.5 where the dc voltage V_{dc} is obtained from a three phase diode rectifier. The load is purely resistive. The third and fifth order harmonics are chosen for experiment in this paper. The dead time is set as 2μs.the equivalent phase shifted angle of dead time is 30^0,10^0, and 6^0 for FPSC, third-order harmonic in HPSC, and fifth-order harmonic in HPSC respectively. The SIMULINK diagram of FPSC or HPSC is shown in fig.13

B. Power Regulation Comparison

Fig.9 shows the voltage measured on load at a given phase shifted angle for three kinds of control methods.

It is known that the curves in fig.9. are very similar with those in fig.7 because the V_{RL} is nearly proportional to V_{pk}. It can be seen that the higher the harmonic order is, the lower the maximum output power is. It is apparently consistent with aforementioned analyses.

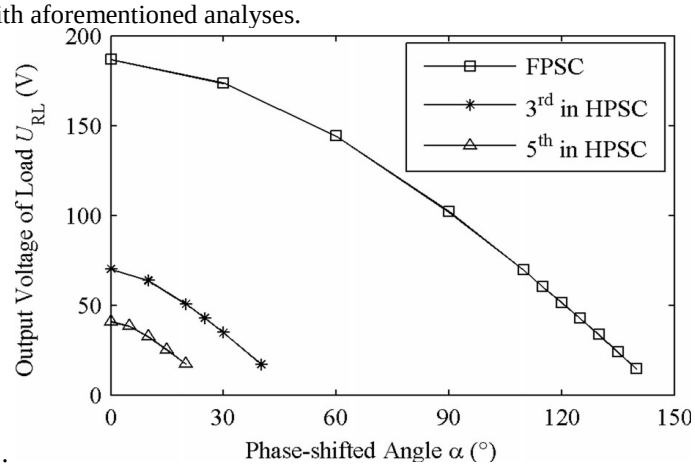

Fig.9. output voltage at different phase-shifted angles with different methods.

The phase shifted angle range is output power for FPSC,the third order harmonic and fifth order harmonic in HPSC is compared. According to the analysis in section III,output power is lower with higher harmonic order, so the reasonable range $1/7^2 \sim 1/5^2$ of normalized output power of the fifth order harmonic in HPSC is selected. According to (14), the start phase shifted angle for the selected normalized power range can be obtained from (19) and the end phase shifted angle is obtained from (20).Then the phase shifted angle range can be calculated

$$G_{PK} = 1/5^2 \ (k = 1,3,5) \qquad (19)$$

$$G_{PK} = 1/7^2 \ (k = 1,3,5) \qquad (20)$$

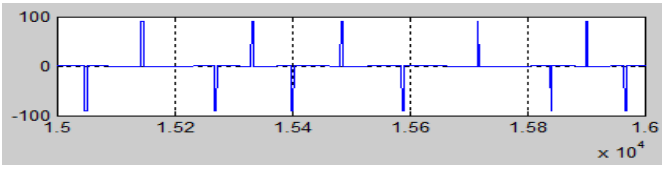

(a)

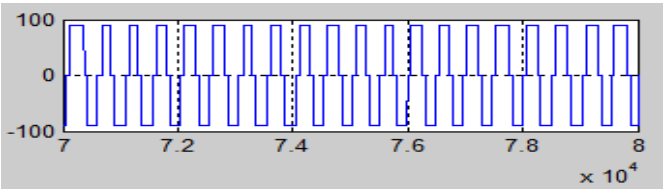

(b)

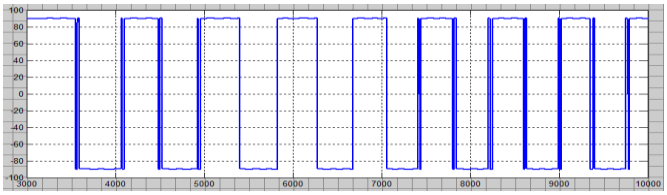

(c)

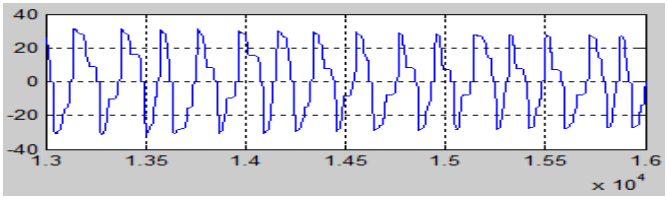

(d)

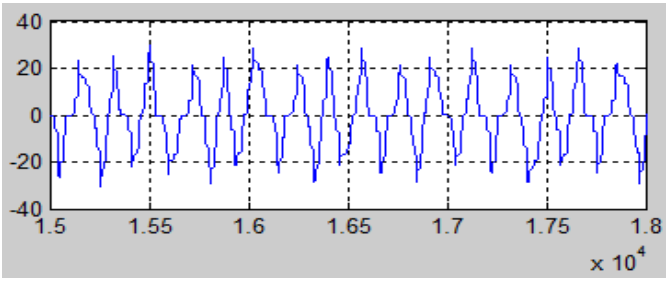

(e)

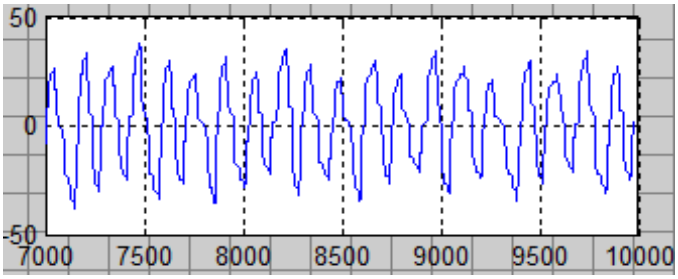

(f)

Fig. 10. Waveforms of inverter output voltage using diff-erent control methods (a) FPSC.(b)third-order harmonic in HPSC. (c) Fifth order harmonic in HPSC. And current using different control methods (d) FPSC. (e) third-order harmonic in HPSC. (f) Fifth order harmonic in HPSC.

A comparison of phase shifted angle range during the same range of normalized output power is shown in table III. From this table it can be known that phase shifted angle range is wider if higher order harmonic is used. The wider phase shifted angle range means higher power regulation accuracy due to the limited digital bits in digital processor.

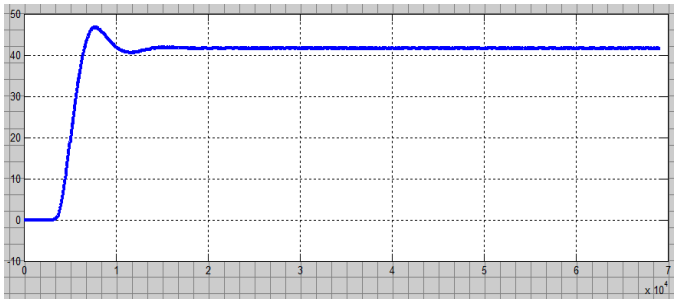

(a)

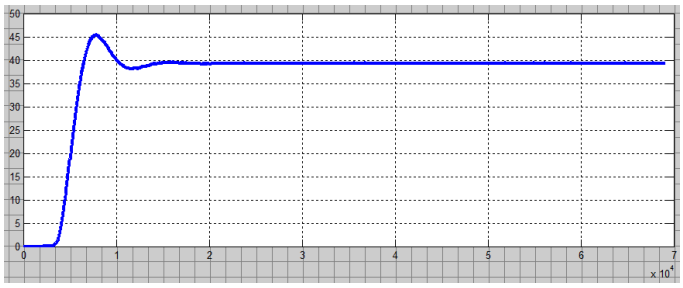

(b)

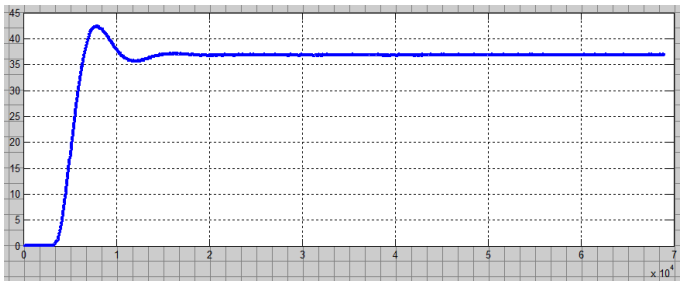

(c)

Fig.11. Waveforms of the rectifier output voltage using different control methods. (a) FPSC. (b) Third-order harmonic in HPSC. (c) Fifth-order harmonic in HPSC.

C. Efficiency Comparison

In order to verify the improvement of system efficiency from HPSC to usual FPSC, experiments for FPSC, the third order harmonic in HPSC, and the fifth order harmonic in HPSC at their power range have all been tested. Here the input power of three phase ac power and load power are measured, and then the normalized value

G_P of output power is expressed as (20).the base value $P_{0max}$is the maximum value of output power at actual zero phase shifted angle using FPSC.The P_{0max}here is 1.77kW.

$$G_P = \frac{P_{out}}{P_{0max}} \qquad (21)$$

Fig.12. shows the efficiency at light load with these three methods. It can be seen that 1) the system efficiency increased with higher output power; 2) system efficiency using HPSC is higher than that of FPSC at the same output power; 3) efficiency of fifth order harmonic in FPSC is higher than that of the third order harmonic in HPSC; and 4) the suitable G_P for HPSC is about less than15% in fact.

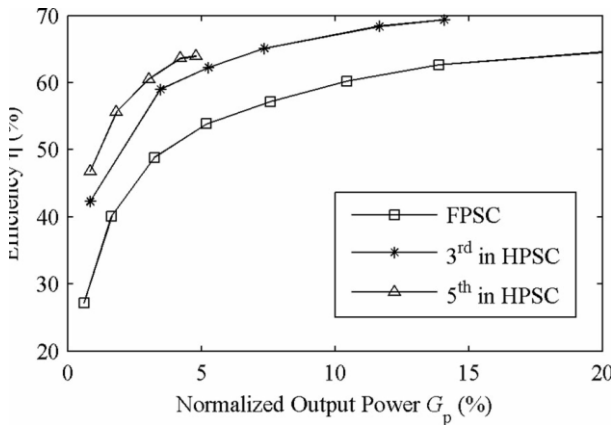

Fig.12. System efficiency with different methods at light load.

D. Comparison under same output power

To compare the proposed HPSC and the conventional FPSC under the same output power, the following experiment is implemented. The output power here is about 88W and G_p is around 5%. Detailed experiment data is shown in table IV. As can be seen from this table the fifth order harmonic in HPSC improves efficiency of system with 10.09% compared to FPSC.It can be inferred that higher efficiency improvement will be reached at lighter load. Fig.10 shows the waveforms of inverter output voltage V_{inv} inverter output current I_P ,and voltage on load V_{RL} with FPSC, the third order harmonic in HPSC,and the fifth order harmonic in HPSC, respectively.fig shows the phase shifted angle is greater at light load for FPSC, which results in great switching losses remarkably. FFT analysis to the inverter output current I_p is carried out to compare the current spectrum, which is shown in fig.14 as can be seen from this figure we have the followings.

Switching frequency adopted by HPSC is much lower than resonant frequency resulting that the low-order harmonic of inverter output voltage takes high proportion.

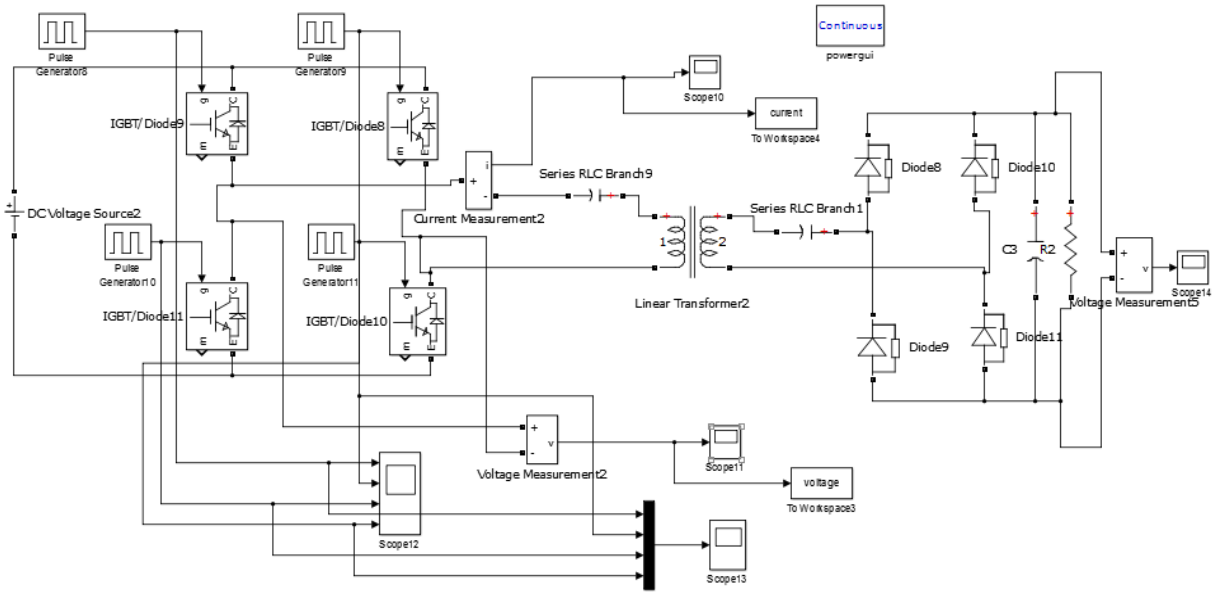

Fig.13. SIMULINK diagram of FPSC or HPSC.

TABLE –III

COMPARISON OF PHASE-SHIFTED ANGLE RANGE UNDER THE SAME RANGE OF NORMALIZED OUTPUT POWER ($1/7^2 \sim 1/5^2$).

Method	Start phase-shifted angle(°)	End Phase-Shifted angle(°)	Phase-shifted angle Range(°)
FPSC	156.9	163.6	6.7
Third-order harmonic in HPSC	35.4	43.1	7.7
Fifth-order harmonic in HPSC	0	17.8	17.8

The amplitude of inverter output current at resonant frequency is almost of the same. The reason is that the power is transferred mainly at the resonant frequency.

1) Low frequency harmonics using HPSC is greater than that of FPSC, whereas high frequency harmonics is lower. This is because the

TABLE-IV

EXPERIMENTAL DATA WITH CONTROL METHODS

Method	f_s(kHz)	α(°)	V_{RL}(v)	η(%)
FPSC	42.0	125	41.58	53.85
Third-order harmonic in HPSC	14.0	25	39.26	62.27
Fifth-order harmonic in HPSC	8.4	0	36.8	63.94

2) If high order harmonic is employed to transfer power for HPSC, there will be more harmonic current components near the resonant frequency. Because the quality factor Q of resonant circuit is not infinite, so the harmonics components far from the resonant frequency are mostly filtered, but those near the resonant

3) frequency do not decay seriously.

Fig.14. FFT analysis of an inverter output current using different control methods.(a)FPSC.(b)Third-order harmonic in HPSC.(c) Fifth-order harmonic in HPSC.

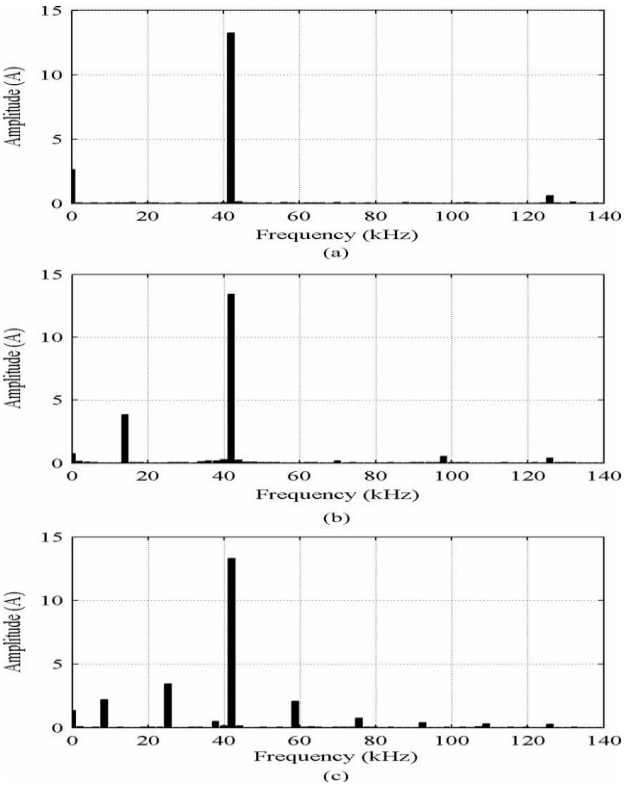

V.CONCLUSION

In this method the switching frequency is set to be much lower than the resonant frequency, but the frequency of selected harmonic component is the same with the resonant frequency. The phase shifted angle of the inverter is controlled to regulate the power. The efficiency increases more than 10% at the light load condition. Analysis and experimental results shows that the proposed method can improve system efficiency compared with the traditional fundamental based phase shifted control. Furthermore improves the power regulation and reduced switching frequency has been achieved simultaneously. Results of the investigation demonstrate that the proposed control method for the resonant converter can effectively improves the converter performance at the light load condition. Because of the characteristics of HPSC that harmonic component is adopted, there is a limited range of normalized output power using HPSC, which is less than11.1% in theory.

REFERENCES

[1] [1] A. K. Swain, M. J. Neath, U. K. Madawala, and D. J. Thrimawithana "A dynamic multivariable state-space model for bidirectional inductive power transfer systems," *IEEE Trans. Power Electron.*, vol. 27, no. 11, pp. 4772–4780, Nov. 2012.

[2] [2] H.Matsumoto, Y. Neba, K. Ishizaka, and R. Itoh, "Model for a three-phase contactless power transfer system," *IEEE Trans. Power Electron.*, vol. 26, no. 9, pp. 2676–2687, Sep. 2011.

[3] [3] Y. Ota, T. Takura, F. Sato, H.Matsuki, T. Sato, and T. Nonaka, "Impedance matching method about multiple contactless power feeding system for portable electronic devices," *IEEE Trans.Magn.*, vol. 47, no. 10, p. 4235—4237, Oct. 2011.

[4] [4] S. Hasanzadeh, S. Vaez-Zadeh, and A.H. Isfahani, "Optimization of a contactless power transfer system for electric vehicles," *IEEE Trans. Veh. Technol.*, vol. 61, no. 8, pp. 3566–3573, Oct. 2012.[5] G. A. J. Elliot, S. Raabe, G. A. Covic, and J. T. Boys, "Multiphase pickupsfor large lateral tolerance contactless power-transfer systems," *IEEE Trans. Ind. Electron.*, vol. 57, no. 5, pp. 1590–1598, May 2010.

[5] [6] J. Kuipers, H. Bruning, S. Bakker, and H. Rijnaarts, "Near field resonant inductive coupling to power electronic devices dispersed in water," *Sens. Actuators A: Phys.*, vol. 178, pp. 217–222, May 2012.

[6] [7] S. Raabe and G. A. Covic, "Practical design considerations for contactless power transfer quadrature pick-ups," *IEEE Trans. Ind. Electron.*, vol. 60, no. 1, pp. 400–409, Jan. 2013.

[7] [8] K. W. Klontz, D. M. Divan, D. W. Novotny, and R. D. Lorenz, "Contactless power delivery system for mining applications," *IEEE Trans. Ind. Appl.*, vol. 31, no. 1, pp. 27–35, Jan./Feb. 1995.

[8] [9] D. J. Hartland, "Electric contact systems – Passing power to the trains," in *Proc. 5th IET Prof. Develop. Course REIS*, London, U.K., 2011, pp. 60–68.

[9] [10] J. Huh, S. W. Lee,W. Y. Lee, G. H. Cho, and C. T. Rim, "Narrow-width inductive power transfer system for online electrical vehicles," *IEEE Trans.Power Electron.*, vol. 26, no. 12, pp. 3666–3679, Dec. 2011.

[10] [11] G. A. Covic, J. T. Boys, M. L. G. Kissin, and H. G. Lu, "A three-phase inductive power transfer system for roadway-powered vehicles," *IEEE Trans. Ind. Electron.*, vol. 54, no. 6, pp. 3370–3378, Dec. 2007.

[11] [12] M. Bauer, P. Becker, and Q. Zheng, "Inductive power supply (IPSR_) for the transrapid," presented at the Magn. Levitated Syst. Linear Drives,Dresden, Germany, 2006.

[12] [13] (Jun. 2012).[Online].Available:http://www.railwaygazette.com/news/urban-rail/si-ngle-view/view/primove-induction-powered-tram-trialproves-

[13] a-success.html

[14] [14] H. H. Wu, G. A. Covic, J. T. Boys, and D. J. Robertson, "A series-tuned indctive-power-transfer pickup with a controllable AC-voltage output," *IEEE Trans. Power Electron.*, vol. 26, no. 1, pp. 98–109, Jan. 2011.

[15] [15] G. B. Koo, G. W. Moon, and M. J. Youn, "Analysis and design of phase shift full bridge converter with series-connected two transformers," *IEEE*

[16] [16] H. L. Li, A. P. Hu, and G. A. Covic, "FPGA controlled high frequency resonant converter for contactless power transfer," in *Proc. IEEE PowerElectron. Spec. Conf. 2008*, Rhodes, Greece, 2008, pp. 3642–3647.

[17] [17] C. S. Tang, Y. Sun, Y. G. Su, S. K. Nguang, and A. P. Hu, "Determining multiple steady-state ZCS operating points of a switch-mode contactless power transfer system," *IEEE Trans. Power Electron.*, vol. 24, no. 2, pp. 416–425, Feb. 2009.

[18] [18] W. P. Choi, W. C. Ho, X. Liu, and S. Y. R. Hui, "Comparative study on power conversion methods for wireless battery charging platform,"in *Proc. EPEPower Electron. Motion Control Conf.*, Ohrid, Republic of Macedonia, 2010, pp. S15-9–S15-16.

[19] [19] J. L. Villa, J. Sallan,A. Llombart, and J.F. Sanz, "Design of a high frequency inductively coupled power transfer system for electric vehicle battery charge," *Appl. Energy*, vol. 86, no. 3, pp. 355–363, Mar. 2009.

[20] [20] C. S. Wang, G. A. Covic, and O. H. Stielau, "Power transfer capabilityand bifurcation phenomena of loosely coupled inductive power transfersystems," *IEEE Trans. Ind. Electron.*, vol. 51, no. 1, pp. 148–157, Feb.2004.

[21] [21] H. Cai, L. M. Shi, and R. H. Zhang, "A novel control method of resonant inverter for movable contactless power supply system of maglev,"presented at the *Int. Conf. Electr. Mach. Syst.*, Beijing, China, 2011.

[22] [22] Hua cai, Liming shi, *Member,IEEE*, and Yaohua Li, " Harmonic –Based Phase-Shifted Control Of Inductively Coupled Power Transfer," *IEEE Trans. Power Electron*, vol.29, no.2, pp. 0885-8993,Feb.2014.

Mr. Gaddala Kaladhar received his B.Tech degree in Electrical and Electronics Engineering from Narasaraopeta Engineering College, Narasaraopeta. Master degree (M.Tech) also from same college. Presently he has been working as Assistant professor in Electrical department since eight years in St. Ann's College of Engineering & Technology, Chirala and pursuing Ph.D from SV University College of Engineering and Technology, SV University, Tirupati.

Mr.Y.Narayana Rao received his B.Tech degree in Electrical and Electronics Engineering from Chundi Ranganayakulu Engineering College, Chilakaluripeta. Master degree (M.Tech) from College of Engineering JNTU, Hyderabad. Presently he has been working as Associate professor in Electrical department since eight years in St.Ann's College of Engineering & Technology, Chirala.

Mr.G.Gopala Rao received his B.Tech degree in Electrical & Electronics Engineering from St.Ann's College of Engineering & Technology, Chirala.